NACA

RESEARCH MEMORANDUM

COMPARISON OF LARGE-SCALE FLIGHT MEASUREMENTS OF ZERO-LIFT DRAG AT MACH NUMBERS FROM 0.9 TO 1.7 OF TWO WING-BODY COMBINATIONS HAVING SIMILAR 60° TRIANGULAR WINGS WITH NACA 65A003 SECTIONS

By Eugene D. Schult

Langley Aeronautical Laboratory
Langley Air Force Base, Va.

[redacted]

CLASSIFIED DOCUMENT

[redacted] affecting the National Defense of the United States within the meaning of the [redacted] mission or the revelation of its contents in any manner to an unauthorized person [redacted]

Information so classified may be imparted only to persons in the military and naval services of the United States, appropriate civilian officers and employees of the [redacted] whose official duties require knowledge thereof, as required by their official duties, and to United States citizens of known loyalty and discretion who [redacted] such knowledge.

NATIONAL ADVISORY COMMITTEE FOR AERONAUTICS

WASHINGTON

October 25, 1950

[redacted]AL

Classification cancelled (or changed to UNCLASSIFIED)

By Authority of NASA Tech Pub Announcement #102
(OFFICER AUTHORIZED TO CHANGE)

By 9Oct56

GRADE OF OFFICER MAKING CHANGE)

4 Apr 61
DATE

NACA RM L50I22

NATIONAL ADVISORY COMMITTEE FOR AERONAUTICS

RESEARCH MEMORANDUM

COMPARISON OF LARGE-SCALE FLIGHT MEASUREMENTS OF ZERO-LIFT DRAG AT MACH NUMBERS FROM 0.9 TO 1.7 OF TWO WING-BODY COMBINATIONS HAVING SIMILAR 60° TRIANGULAR WINGS WITH NACA 65A003 SECTIONS

By Eugene D. Schult

SUMMARY

An investigation of zero-lift drag of a fin-stabilized wing-body combination was made at high-subsonic and supersonic speeds in the Reynolds number range of 13×10^6 to 41×10^6. The ratio of body frontal area to wing area was 0.0612. These data are presented with those of a wingless body and similar winged body described in NACA RM L50D26 in which the ratio of body frontal area to wing area was 0.0306. The bodies of both configurations were the same as the wingless body and had parabolic profiles and fineness ratios of 10. The wings were triangular in plan form with a leading-edge sweep of 60° and NACA 65A003 airfoil sections.

The results indicated that the small-winged combination with two fins had a total drag coefficient of 0.01 at subsonic speeds and 0.018 to 0.015 at supersonic speeds. Wing-plus-interference drag coefficient varied from 0.006 at high-subsonic speeds to 0.01 at transonic speeds and 0.005 at supersonic speeds.

A comparison of results with a similar configuration having twice the wing area indicated that the small-winged body had a greater wing-plus-interference drag coefficient in the subsonic and transonic range and approximately equal drag coefficient in the supersonic range. The mutual interference effects were unfavorable for the small-winged configuration and favorable for the large-winged configuration. The base pressure coefficients for the small-winged body changed from approximately zero at subsonic speeds to -0.075 at supersonic speeds. Doubling the wing area increased the absolute pressures at the base and correspondingly reduced the base drag. This drag, however, represented a very small part of the total drag of the configuration.

INTRODUCTION

As part of its program on transonic research, the Langley Pilotless Aircraft Research Division is conducting a series of free-flight tests at high Reynolds numbers to determine the zero-lift drag characteristics of several winged-body configurations. These tests employ the rocket-powered model technique and provide continuous data from supersonic to high-subsonic speeds.

The primary objective of this series of investigations is to study low-drag configurations at transonic and supersonic speeds. A triangular wing with NACA 65A003 sections was combined with a parabolic body of fineness ratio 10. One configuration of this series has already been flown; it had twice the wing area of the present test model and its results as well as those of a wingless body were reported in reference 1 and are included in this paper to determine the effect of wing size relative to the body on the drag characteristics. Previously unpublished base-pressure data for the large-winged and wingless models are also presented.

The Mach number range for the present test was from 0.9 to 1.7, and the Reynolds number based upon a mean aerodynamic chord of 3.42 feet varied from approximately 13×10^6 to 41×10^6.

SYMBOLS

C_D drag coefficient based on total included wing area

C_{p_b} body base pressure coefficient, $\left(\frac{p_b - p}{q}\right)$

C_{D_b} body base drag coefficient based on body frontal area, $\left(C_{p_b}(S_b/S_f)\right)$

p_b body base pressure, pounds per square foot

p atmospheric pressure, pounds per square foot

q dynamic pressure, pounds per square foot, $(\gamma p M^2/2)$

γ specific-heat ratio, 1.40 for air

[redacted]

[redacted]

M	Mach number (V/c)
V	model velocity, feet per second
c	velocity of sound, feet per second, $(49.25\sqrt{T})$
T	absolute temperature, degrees Rankine
S_b	body base area, 0.228 square foot
S_f	body frontal area, 0.922 square foot
R	Reynolds number based on wing mean aerodynamic chord

MODEL AND TESTS

The present test body, the same as that described in reference 1, had a profile formed by parabolic arcs each having its vertex at the maximum diameter, which was located at the 40-percent body station. The ratio of body length to maximum diameter was 10, the ratio of body frontal area to total included wing area was 0.0612, and the ratio of stern base area to total included wing area was 0.015.

Figure 1 illustrates the general arrangement of the configuration and also shows the larger wing outline from reference 1. The 50-percent-wing-root-chord point was located at body station 78.00 inches for the large-winged and small-winged combinations. Station 78.00 corresponds to the 60-percent body station and was selected in this case to maintain a consistency in wing location with other wing plan forms tested.

The triangular wing had a leading-edge sweep of 60° and NACA 65A003 airfoil sections parallel to the longitudinal center line of the model. Rounding off the tips for structural reasons resulted in a total included area of 15.13 square feet or a reduction of approximately 1/2 percent from that of the basic triangular plan form. Exposed wing area was 10.81 square feet. The corresponding total and exposed areas for the wing reported in reference 1 were 30.28 and 24.02 square feet, respectively. Wing and body coordinates are listed in table I.

The two vertical stabilizing fins were made of magnesium and had sections as illustrated in figure 1. They were the same as those used on the large-winged body with two fins and on the wingless body with four fins. A Deacon rocket motor, rated at a nominal thrust of 5700 pounds for 3.5 seconds, propelled the model to its peak velocity.

[redacted]

Doppler radar was used to obtain velocity and acceleration data which were reduced to drag coefficients by the method described in reference 2. A continuous time history of longitudinal accelerations telemetered to the ground station provided an independent means for substantiating Doppler drag data. A trajectory was obtained with SCR 584 radar and the necessary atmospheric data from radiosonde observations. Base pressure coefficients were derived from a survey of ambient pressures and telemetered values of pressure at the base periphery. Details of the stern base section are shown in figure 2, and a general view of the test model on the launching stand is reproduced in figure 3.

The variation of Reynolds number with Mach number is presented in figure 4 for this test configuration and for the winged-body and wingless-body configurations reported in reference 1. The curves are based upon both body length and upon the wing mean aerodynamic chord of the model it represents.

ACCURACY

The accuracy of the test results is estimated to be within the following limits:

Mach number	±0.005
Total drag coefficient based on wing area of 15.13 sq ft	±0.0010
Base pressure coefficients:	
At M = 1.3	±0.01
At M = 1.0	±0.02
At M = 0.9	±0.03

The values listed for drag and base pressure coefficients are absolute accuracies. Relative values and trends for any one curve are believed to be more accurate.

RESULTS AND DISCUSSION

Total Drag

Plots of zero-lift drag coefficients based on total included wing area are presented as a function of Mach number in figures 5(a) and 5(b) for the large-winged and the small-winged configurations, respectively. The drag coefficients for the wingless body have been taken from reference 1 and are shown for comparison in figures 5(a) and 5(b);

these data represent the drag of a two-finned wingless body, based upon the respective total wing area. Also shown in figures 5(a) and 5(b) are the variations of base drag coefficient with Mach number for the winged combinations. The base drag coefficients are referred to the total wing area of the respective configuration and are derived from values of base pressure measured at the base periphery.

The present test results (fig. 5(b)) show a subsonic drag coefficient of 0.01 with the force-break Mach number occurring at 0.96; at supersonic speeds the drag coefficients decreased from 0.0182 at a Mach number of 1.05 to 0.0152 at a Mach number of 1.75. Slight dips in the drag curves of the winged bodies near the force-break Mach number were revealed by continuous-line telemeter records of longitudinal accelerations. The cause of these dips and whether they bear a relationship to those in base drag is not understood; the Mach number difference of 0.01 in this case does not seem to be an error since records of accelerations and base pressures were recorded simultaneously on the same film.

Wing-Plus-Interference Drag

The wing-plus-interference drag coefficients shown in figure 5(c) were obtained by subtracting the total drag of the wingless body from the total drag of the winged bodies. The wing-plus-interference drag coefficients for the small-winged present test configuration are approximately 0.006 at subsonic and 0.005 at supersonic speeds. The results at supersonic speeds agreed closely with those of the larger-winged model and indicate that the coefficients increase only slightly with area. This analysis, however, does not distinguish between the small differences in base drag, and a slightly greater spread between the wing-plus-interference curves can be expected at supersonic speeds when the effect of base drag is taken into account.

At transonic speeds, the over-all drag in pounds was highest for the small-winged configuration and the divergence of the curves is largely the result of a lower drag-rise Mach number of the small-winged body with respect to that of either the body alone or the large-winged body. These differences in drag-rise Mach number indicate a critical interaction of flows induced by the wing and body which is favorable for the larger wing and unfavorable for the smaller wing. An experimental investigation of the effect of location of an untapered 45° swept wing on total drag was reported in reference 3, and it was found that a wing location rearward of maximum body diameter reduced the drag considerably. From the results of the present test, however, it becomes apparent that the location of the wing leading edge rearward of the maximum diameter is not sufficient to assure a low over-all drag.

[redacted]

Figure 6(a) presents the variations of base pressure coefficient with Mach number for the three configurations; these values represent a mean of pressures at the base circumference which according to unpublished data are slightly less positive than coefficients representative of the whole base. The differences in the trends of C_{p_b} with Mach number between center and edge orifices were small and for this test would have little effect on the over-all drag coefficient of the combination.

Base pressure coefficients for the wingless body are approximately zero near $M = 0.95$ and change to approximately -0.08 at supersonic speeds. The winged bodies had more positive pressure coefficients at supersonic speeds than the wingless body with four tail fins by 0.02 for the smaller-winged body and by 0.10 for the larger-winged body. At subsonic speeds the change of base pressure coefficients with body configuration was much less. The Reynolds number of the large-winged body (fig. 4) was slightly different from that of either the small-winged body or the body alone with four tail fins when Reynolds numbers are based on body length, and the possibility exists that a change in boundary-layer characteristics in the vicinity of the base may have influenced the magnitude of base edge pressures to some extent.

Base drag coefficients, referred to body frontal area, are shown in figure 6(b) and are equal to the product of pressure coefficient (fig. 6(a)) and the ratio of base area to frontal area of the body. The base drag at supersonic speeds averaged approximately 10 percent of the total drag of the wingless body, 6 percent of the drag of the small-winged configuration, and less than 2 percent for the large-winged configuration.

CONCLUDING REMARKS

An investigation of zero-lift drag of a fin-stabilized wing-body combination was made at high-subsonic and supersonic speeds and at Reynolds numbers from 13×10^6 to 41×10^6. The 60° triangular wing had NACA 65A003 sections and the ratio of body frontal area to wing area was 0.0612. The body had a parabolic profile and a fineness ratio of 10. The combination was similar to but had one-half the wing area of the model described in NACA RM L50D26.

The results indicated that the present small-winged configuration had a total drag coefficient of 0.01 at subsonic speeds and 0.018 to 0.015 at supersonic speeds. Wing-plus-interference drag coefficient varied from 0.006 at high-subsonic speeds to 0.01 at transonic speeds and 0.005 at supersonic speeds.

[redacted]

A comparison of these results with the large-winged configuration indicated that the small-winged body had a greater wing-plus-interference drag coefficient in the subsonic and transonic range and approximately equal drag coefficient in the supersonic range. At transonic speeds, the small-winged body had greater over-all drag and more unfavorable interference compared to the larger-winged body.

The base pressure coefficients for the small-winged body changed from approximately zero at subsonic speeds to -0.075 at supersonic speeds. Doubling the wing area increased the absolute pressures at the base and correspondingly reduced the base drag. This drag, however, was a very small part of the total drag of the configuration.

Langley Aeronautical Laboratory
National Advisory Committee for Aeronautics
Langley Air Force Base, Va.

REFERENCES

1. Nelson, Robert L.: Large-Scale Flight Measurements of Zero-Lift Drag at Mach Numbers from 0.86 to 1.5 of Wing-Body Combination Having a 60° Triangular Wing with NACA 65A003 Sections. NACA RM L50D26, 1950.

2. Morrow, John D.: Measurements of the Effect of Trailing-Edge Thickness on the Zero-Lift Drag of Thin Low-Aspect-Ratio Wings. NACA RM L50F26, 1950.

3. Mathews, Charles W., and Thompson, Jim Rogers: Comparison of the Transonic Drag Characteristics of Two Wing-Body Combinations Differing Only in the Location of the 45° Sweptback Wing. NACA RM L7I01, 1947.

[redacted]

TABLE I

BODY AND WING COORDINATES FOR TEST MODELS

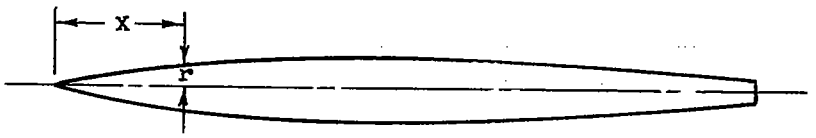

Body coordinates 130-inch parabolic model (in.)			
X	r	X	r
0	0	54.60	6.496
.78	.194	62.40	6.442
1.17	.289	70.20	6.322
1.95	.478	78.00	6.137
3.90	.938	85.80	5.886
7.80	1.804	93.60	5.570
11.70	2.596	101.40	5.188
15.60	3.315	109.20	4.742
23.40	4.534	117.00	4.229
31.20	5.460	124.80	3.652
39.00	6.094	130.00	3.230
46.80	6.435		

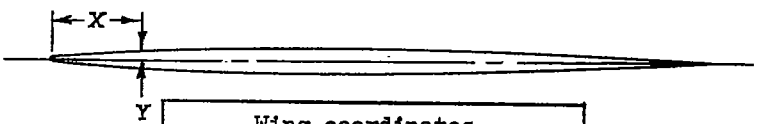

Wing coordinates NACA 65A003 (percent chord)			
X	Y	X	Y
0	0	40	1.498
.50	.232	45	1.496
.75	.282	50	1.463
1.25	.359	55	1.397
2.50	.491	60	1.303
5.00	.657	65	1.182
7.50	.796	70	1.044
10.00	.912	75	.888
15.00	1.097	80	.719
20.00	1.237	85	.545
25.00	1.344	90	.364
30.00	1.421	95	.185
35.00	1.473	100	.007
L.E. radius = 0.115c T.E. radius = 0.007c			

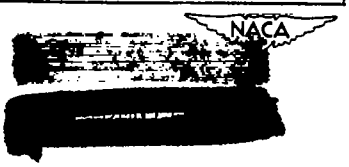

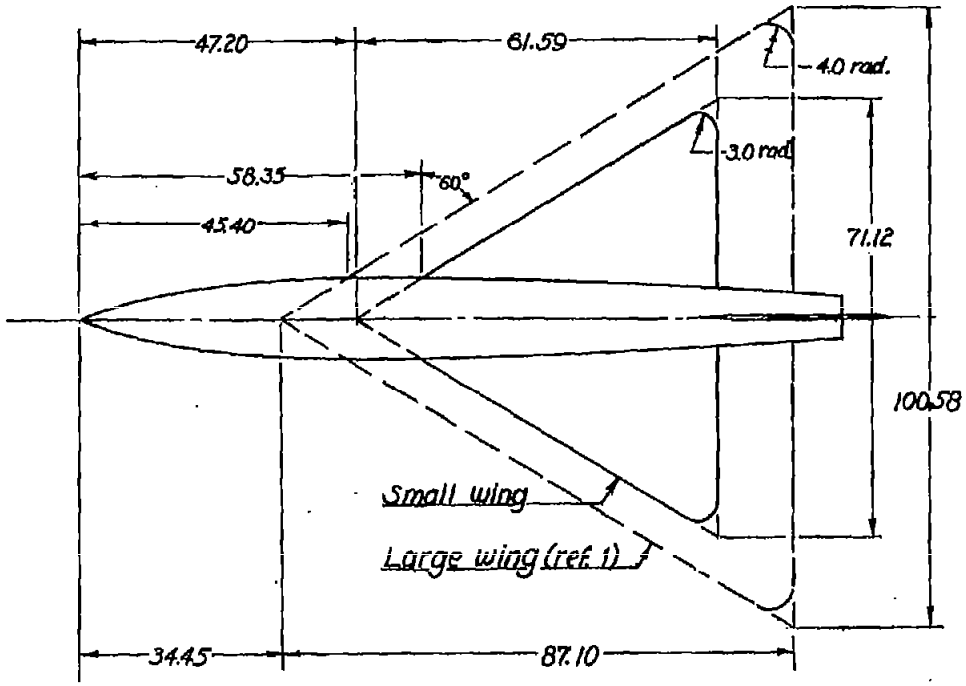

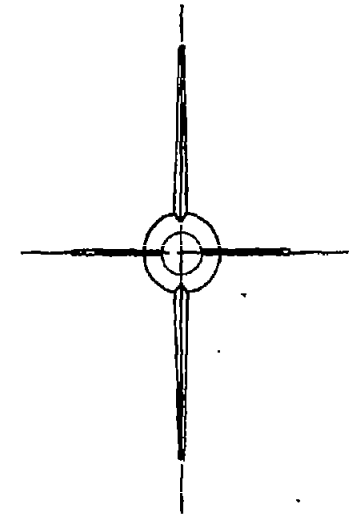

All dimensions in inches.

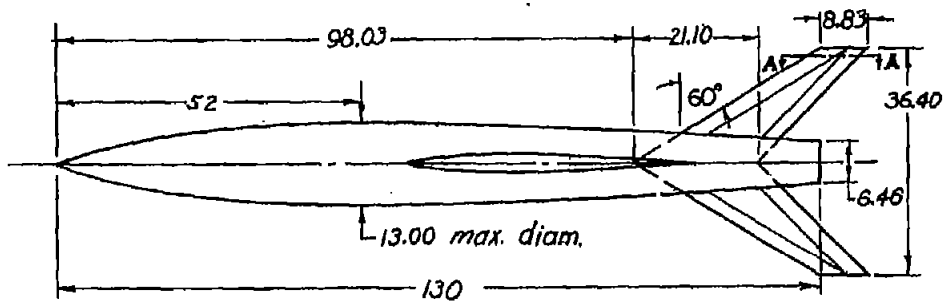

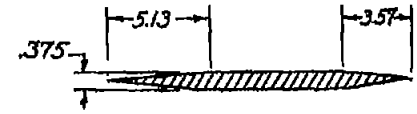

Typical fin section A-A

NACA

Figure 1.- General arrangement of test model. Locations of large and small wings are shown.

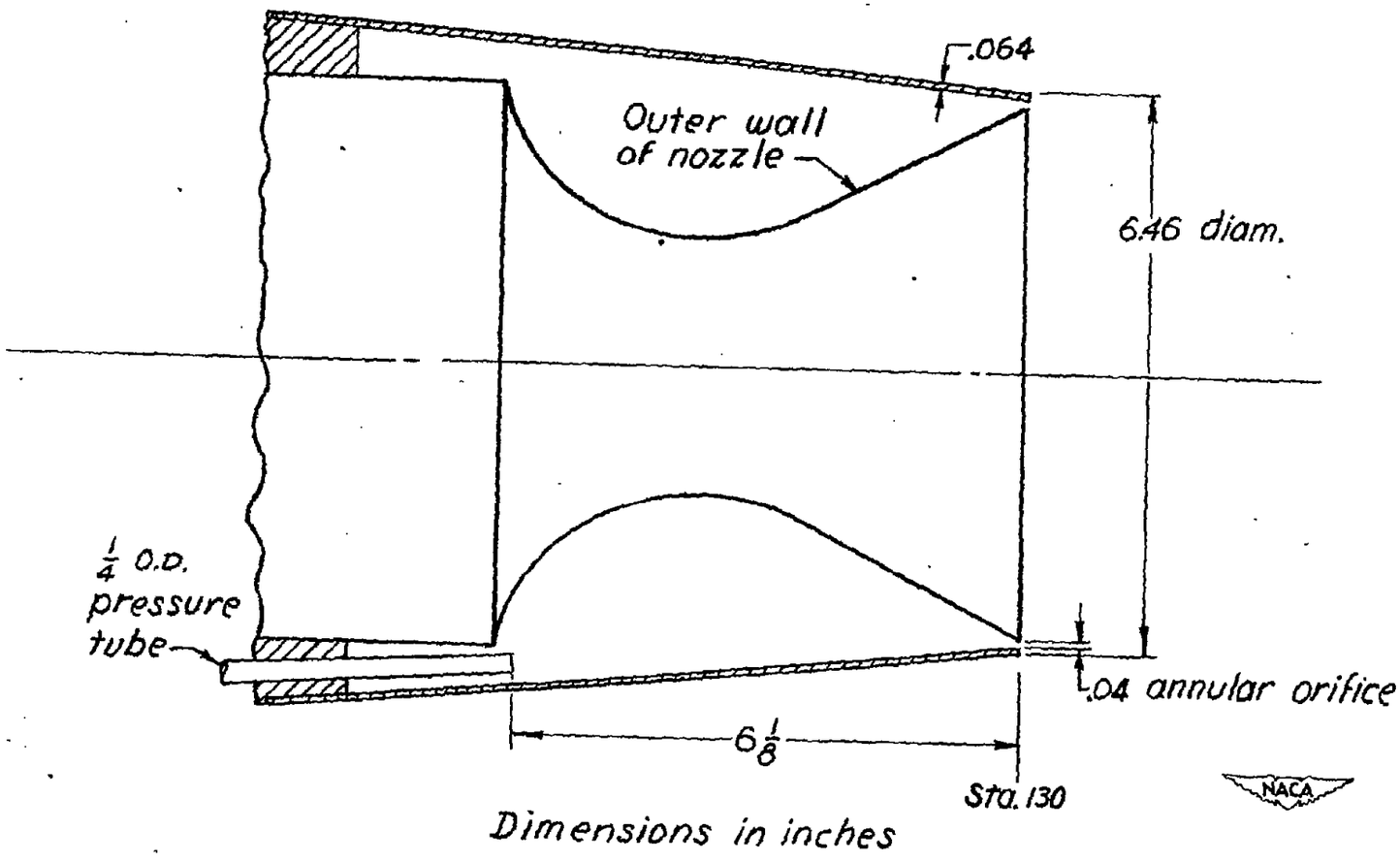

Figure 2.- Sketch of body base-pressure-tube installation.

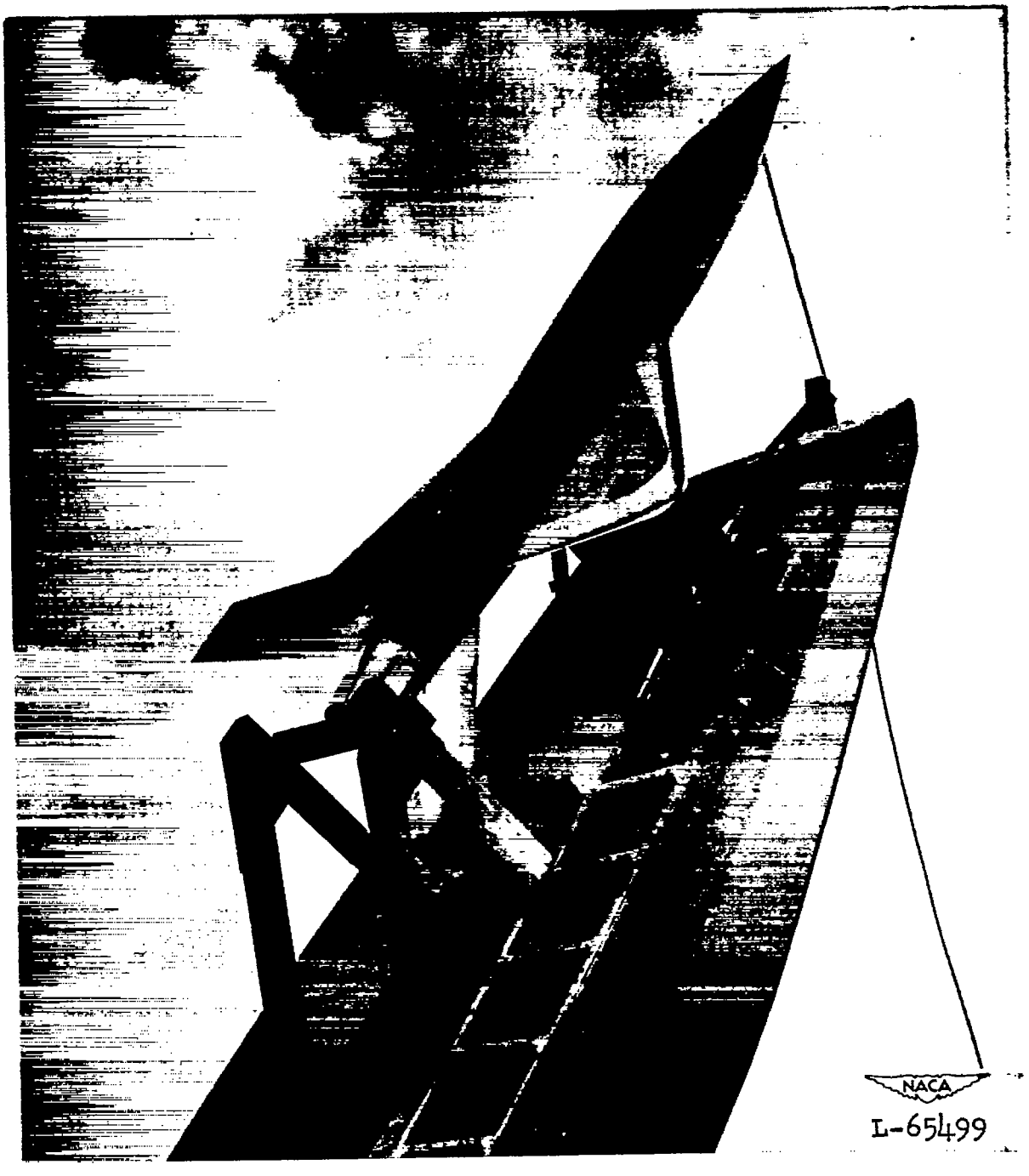

Figure 3.- General view of the small-winged test model on the launching stand.

[redacted]

[redacted]

[redacted]

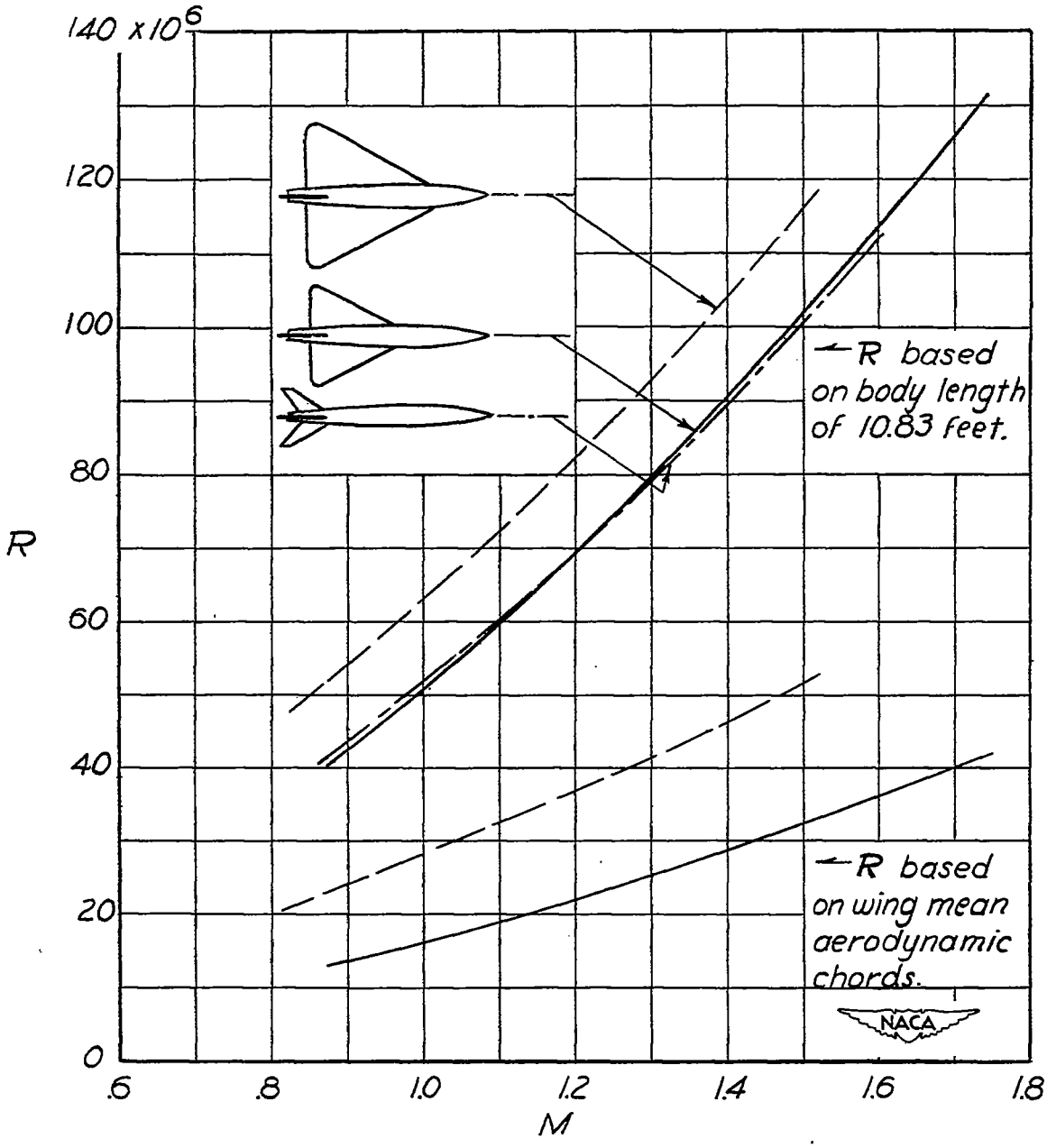

Figure 4.- Variation of Reynolds number with Mach number for test models. Mean aerodynamic chords were 3.42 feet and 4.84 feet.

[redacted]

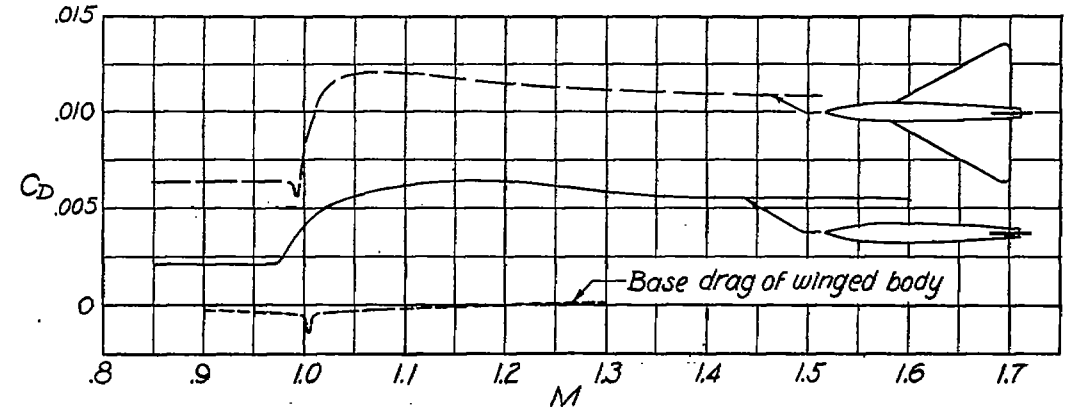

(a) Large-winged body (reference 1).

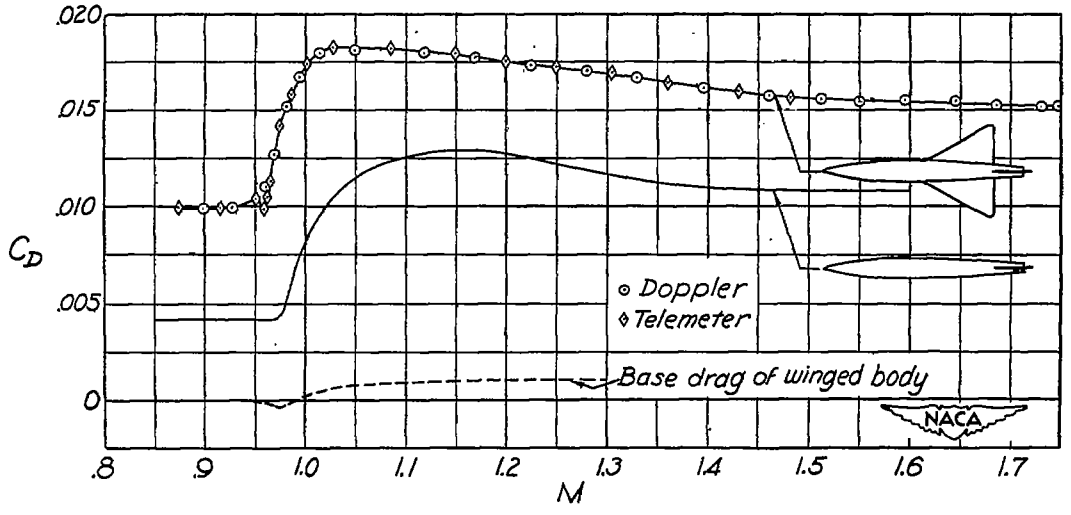

(b) Small-winged body (present test).

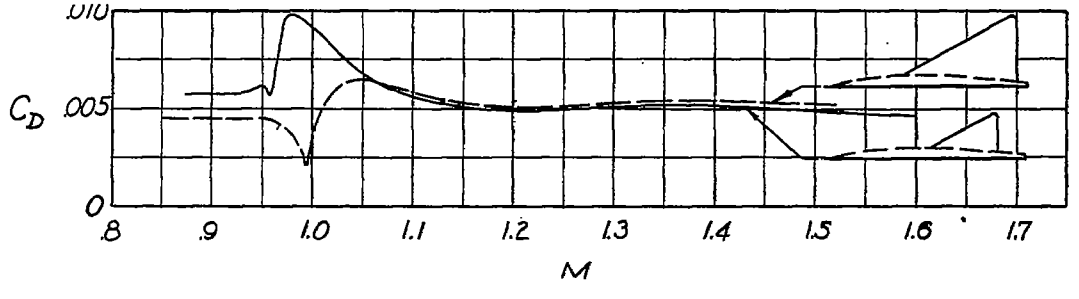

(c) Wing plus interference.

Figure 5.- Variation of drag coefficient with Mach number. Coefficients are based on total included wing area.

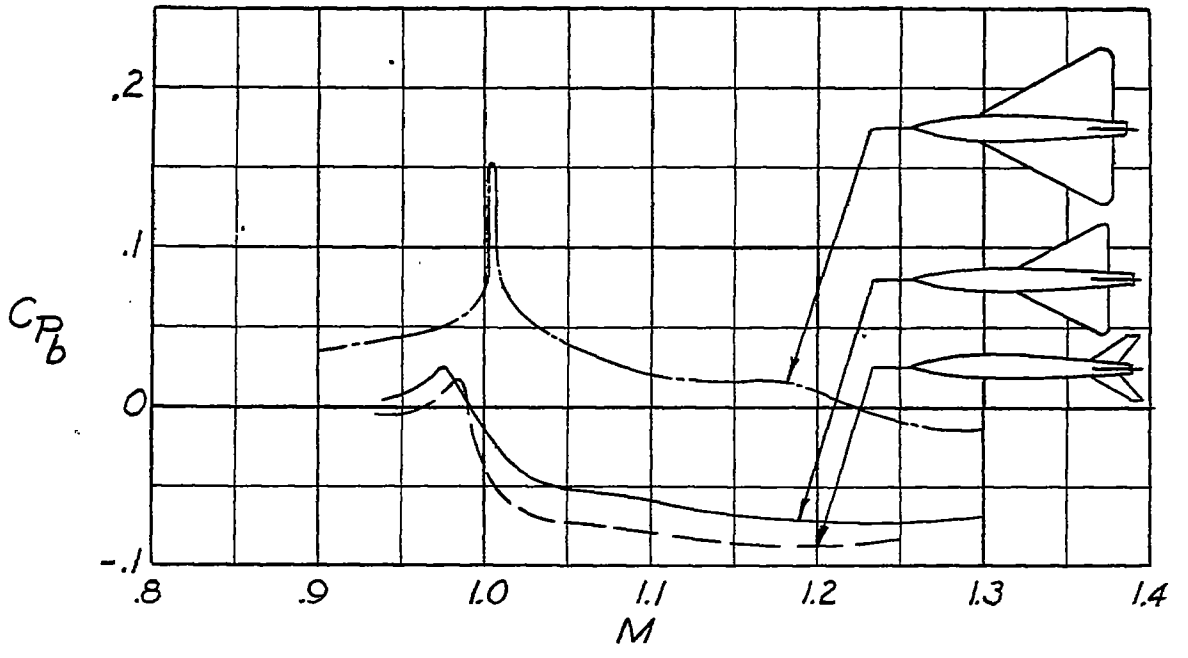

(a) Base pressure.

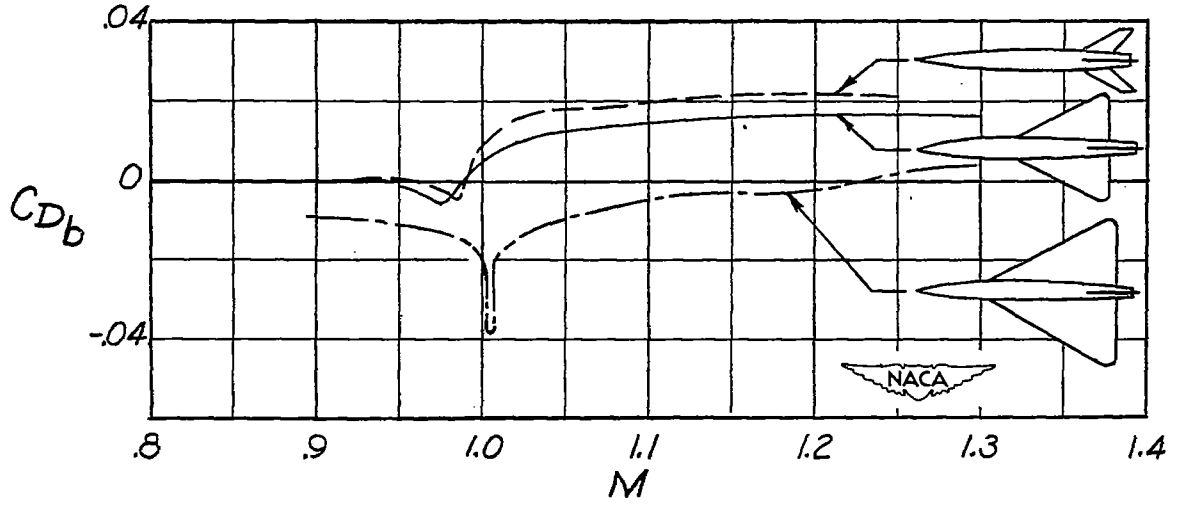

(b) Base drag.

Figure 6.- Variation of base pressure coefficient and base drag coefficient with Mach number for two wing-body configurations of different wing areas and for a body alone with four tail fins. Base drag coefficient is based upon a body frontal area of 0.922 square feet.

[redacted]